Hybrid Materials

DOI: 10.1002/anie.201105496

ECS-3: A Crystalline Hybrid Organic–Inorganic Aluminosilicate with Open Porosity

*Giuseppe Bellussi, Erica Montanari, Eleonora Di Paola, Roberto Millini, Angela Carati, Caterina Rizzo, Wallace O'Neil Parker Jr., Mauro Gemmi, Enrico Mugnaioli, Ute Kolb, and Stefano Zanardi**

The synthesis of aluminosilicate hybrids with organic groups fused within a crystalline framework is a daunting mission which has eluded many workers. Hybrids add variable chemical modification to the repertoire of zeolites, which are well established as heterogeneous catalysts, ion exchangers, and molecular sieves with many different pore architectures.[1]

Until the discovery of the crystalline ECSs (eni carbon silicates),[2] only amorphous siliceous fully hybrid materials were known. These, referred to as periodic mesoporous organosilicas (PMOs), are related to well known M41S materials with arrays of mesopores surrounded by pseudo-ordered organosilica walls.[3] Partial incorporation of organic groups into zeolites was first reported by Davies and Wight, who used a reactant mixture of silsesquioxane together with a conventional silica source (e.g., tetraethyl orthosilicate).[4] This approach has strong limitations. It can only be applied to zeolites with metal cations (e.g., NaX) or prepared using organic structure-directing agents that can be extracted by ion exchange (e.g., Beta) to avoid high-temperature treatment, which is deleterious for the organosilico group.[4] Grafting silsesquioxanes onto preformed zeolites failed because most of the SiOH groups are located in the intercrystalline mesoporous regions.[5]

A more successful approach for synthesizing hybrid zeolites involves using bis-silylated organic precursors of general formula $(R'O)_3Si{-}R{-}Si(OR')_3$ ($R = CH_2$, CH_2CH_2; $R' = CH_3$, CH_2CH_3) as silica source.[6–8] However, the much lower than expected organic content indicates that the Si–C bonds undergo hydrolysis. In any case, incorporation of methylene groups within the zeolite framework (an isomorphous substitution of –O– by $-CH_2-$) is still debated because of the impossibility to distinguish a methylene group in the framework from one in the amorphous impurities that are usually present.[8]

A breakthrough in the synthesis of crystalline aluminosilica-based hybrid organic–inorganic porous materials occurred in 2008 with the advent of ECS.[2] ECS synthesis resembles that of PMOs (i.e., low crystallization temperature and bis-silylated organic precursors as silica source), except that no surfactants are used and $NaAlO_2$ is the source of aluminum. ECS-2, prepared with 1,4-bis(triethoxysilyl)benzene, was the first structure to be resolved.[2] It consists of a regular stacking of aluminosilicate and organic layers, the latter made up of phenylene groups covalently bound to the Si atoms of adjacent inorganic layers. Formally, ECS-2 can be classified as clathrasil-like, since the arrangement of the phenylene rings generates large cages disconnected from the exterior.[2]

We now report the structure of another ECS: ECS-3 has textural properties typical of a crystalline microporous material (specific surface area $296\ m^2 g^{-1}$, specific pore volume $0.13\ cm^3 g^{-1}$, type I N_2 adsorption isotherm; see Supporting Information, Figure S1). NMR analysis showed that nearly all of the silicon atoms in ECS-3 are bonded to one carbon atom and three OAl groups (^{29}Si signals at −65 and −68 ppm; Supporting Information, Figures S2 and S3 and Table S1), and the aluminum nuclei are AlO_4 sites (^{27}Al signal at 53 ppm).[2]

The crystal structure solution of ECS-3 proved to be most challenging. In fact, its polycrystalline nature with invariably small crystals ($\leq 1\ \mu m$), the highly complex high-resolution X-ray powder diffraction (HR-XRPD) pattern, even from a synchrotron beam line, and the extremely fast deterioration of the structure under the electron beam of a transmission electron microscope prevented us from applying conventional methods. Even the most advanced approaches failed, for example, HR-XRPD combined with HRTEM and precession electron diffraction (PED), which recently allowed the structures of complex zeolite phases such as TNU-9,[9] IM-5, and SSZ-74 to be determined.[10,11]

The innovative automated diffraction tomography (ADT) technique was able to surmount these obstacles. ADT collects electron-diffraction data from a single small ($< 1\ \mu m$) non-oriented crystal by tilting around an arbitrary axis.[12] The mild electron dose allows data collection on beam-sensitive materials. Moreover, ADT data are less affected by dynamic scattering than conventional in-zone diffraction data, as

[*] Dr. G. Bellussi, Dr. E. Montanari, Dr. E. Di Paola, Dr. R. Millini, Dr. A. Carati, Dr. C. Rizzo, Dr. W. O'Neil Parker Jr., Dr. S. Zanardi
eni s.p.a.—Refining & Marketing Division
Via F. Maritano 26, 20097 San Donato Milanese (Italy)
E-mail: stefano.zanardi@eni.com
Dr. M. Gemmi
Dipartimento di Scienze della Terra "A. Desio"
Università degli Studi di Milano
Via Botticelli 23, 20133 Milano (Italy)
and
Center for nanotechnology innovation@NEST Istituto Italiano di Tecnologia, Pisa (Italy)
Dr. E. Mugnaioli, Prof. U. Kolb
Institut für Physikalische Chemie, Universität Mainz
Welderweg 11, 55099 Mainz (Germany)

Supporting information for this article is available on the WWW under http://dx.doi.org/10.1002/anie.201105496.

confirmed by success with complex inorganic and organic materials.[13]

Analysis of ADT data collected on a small ECS-3 crystal (Supporting Information, Figure S4) under stable conditions (see Table 1 for details) delivered a monoclinic unit cell: $a = 19.7$, $b = 27.7$, $c = 9.5$ Å; $\beta = 102.7°$. Careful inspection of the systematic extinctions revealed the possible space groups to be $C2/c$ or the corresponding acentric Cc.

Table 1: Summary of the ADT data set employed for structure determination of ECS-3.

data type	ADT
tilt range [°]	120°
total reflections	6241
independent reflections	2206
resolution [Å]	1.0
reflection coverage [%]	83
R sym [%]	16.2
SIR 2004 final *R* [%]	24.7

The unit-cell composition was determined by combining the analytical data collected on several single crystals by SEM/EDS and by thermogravimetric (TG) analysis of the bulk sample. The composition differed somewhat from that derived from the elemental analysis reported by Bellussi et al.[2] In fact, the Si/Al ratio was invariably close to 1.3 instead of 1.07, while the Na/K ratio was much higher (8.5 vs. 3.3) (Table 2). These results strongly indicate that the bulk sample contains a minor amorphous phase rich in Al and K.

Based on intensities extracted from 3D electron-density data (ADT), a significant portion of the ECS-3 structure was readily obtained by using Cc space group in the SIR2004 software suite.[14] The phenylene rings were completed with the specific routines of SIR2004, while the position of the extraframework species (Na/K and H_2O) were determined by analysis of the Fourier maps generated during the Rietveld refinement of the structure performed against the HR-XRPD data with GSAS software.[15] Refinement was done by assuming only Na ions and neglecting K, a reasonable approximation considering the complexity of the HR-XRPD pattern and the high Na/K ratio. It converged to low discrepancy factors (Table 2) with fine agreement between experimental and calculated patterns (Supporting Information, Figure S5). Interestingly, the refined Si/Al ratio (1.33) was very close to the value determined by SEM/EDS (1.3, Table 2).

Table 2: Crystallographic data and experimental conditions for the Rietveld refinement of ECS-3.

refined structure	$Na_{20.8}Si_{32}Al_{24}O_{96}C_{96}{\cdot}32\,H_2O$
chemical and TG analyses	$Na_{23}K_7Si_{32}Al_{30}O_{96}C_{96}{\cdot}50\,H_2O$
EDS and TG analyses[a]	$Na_{22.1}K_{2.6}Si_{32}Al_{23.7}O_{96}C_{96}{\cdot}50\,H_2O$
space group	*Cc*
a [Å]	19.7678(5)
b [Å]	28.3299(6)
c [Å]	9.7622(2)
β [°]	104.18(1)
V [Å^3]	5300.4(2)
RF^2 [%]	8.0
Rp [%]	6.0
Rwp [%]	7.8
min./max. residual electron density [e A^{-3}]	−0.465/0.458
no. of observations	16196
no. of reflections	6547
no. of parameters	247
no. of geometrical restraints	196

[a] C content from chemical analysis.

Similarly to ECS-2,[2] the structure of ECS-3 can be described by stacking along the [100] direction of aluminosilicate layers lying on the (001) plane and held together by phenylene groups (Figure 1). The inorganic layers are built up

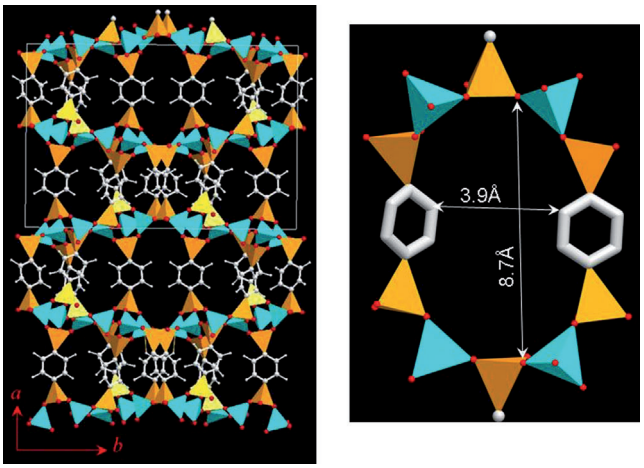

Figure 1. Left: [001] projection of the ECS-3 framework structure. H positions were calculated by geometry optimization (Al turquoise, Si yellow, C white, O red). Right: ellipsoidal ring of the sinusoidal channel snaking along [001]. H atoms are omitted for clarity.

by zeolitic 4=1 secondary building units (SBU) interconnected by additional four-membered rings (4MR, Figure 2a and b) such that two crystallographically independent 8MR, with free dimensions of 5.5×2.3 and 4.8×2.7 Å, respectively, are formed (Figure 2c).

The open porosity is not due to these 8MRs, as evidenced by inspecting the structure along the [001] direction (Figure 1). In this direction elliptical rings are composed of ten tetrahedra and two phenylene rings (Figure 1). The accessibility of these elliptical rings is limited by the steric hindrance imposed by the phenylene rings which, lying on different planes, reduce the free diameter to approximately 8.7×3.9 Å. As a consequence of the noncoplanar arrangement of the phenylene rings, a sinusoidal channel snakes along the crystallographic c direction, forming large side pockets which alternate along the [010] direction on both sides of the channel (Figure 3). The aperture of the side pockets is again composed of ten tetrahedra and two phenylene rings, but the ring is more circular and the arrangement of the phenylene does not reduce the free dimensions of the ring, estimated to be 9.4×7.3 Å (Supporting Information, Figure S6).

The high aluminum content (Si/Al = 1.3) of ECS-3 complicates ion exchange to generate the H^+-form acid

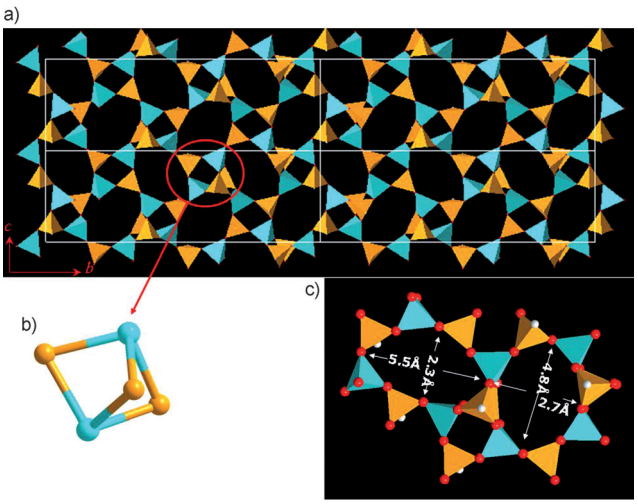

Figure 2. a) Inorganic layer viewed along [100]. b) Ball-and-stick representation of the 4=1 SBU. Oxygen atoms are omitted for clarity and sticks represent the T–T bonds. c) Polyhedral representation of the two 8MRs of the inorganic layer. Al turquoise, Si yellow, C white, O red.

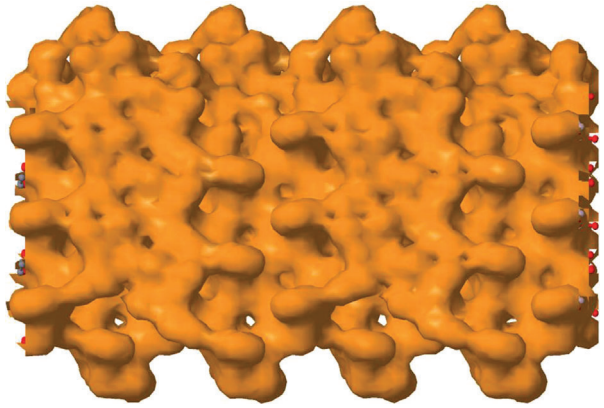

Figure 3. Envelope representation of ECS-3 structure viewed along [100]. The sinusoidal channel runs parallel to the [001] direction, and the side pockets develop along the [010] direction.

catalyst. Attempts will be made to reduce the framework aluminum content. In the meantime, several applications are being studied for this strongly basic catalyst.

In conclusion, ECS-3 confirms the synthesis of microporous crystalline organic–inorganic aluminosilicate hybrids. In particular, ECS-3 is the first such hybrid with open microporosity produced by a regular arrangement of inorganic and organic layers. The intriguing crystal structure of ECS-3, whose framework contains 62 atoms in the asymmetric unit, is one of the most complex structures ever solved by electron diffraction, with a structural complexity comparable to zeolites like ITQ-22.[16] This is remarkable considering the high beam sensitivity of the sample, due to the phenylene rings. ADT was indeed indispensable and could become widely utilized for structural investigation of hybrid nanocrystalline microporous materials.

Experimental Section

ECS-3 was synthesized according to the procedure reported by Bellussi et al.,[2] by using 1,4-bis(triethoxysilyl)benzene and sodium aluminate ($NaAlO_2$) as silica and alumina sources, respectively, KOH, NaOH, and demineralized water. The hydrothermal treatment of the reactant mixture, charged in a stainless steel autoclave, was performed at 373 K for 14 d under autogenous pressure. Once cooled to room temperature, the solid product was collected by filtration, washed with demineralized water, and dried overnight at 373 K. Nitrogen adsorption/desorption isotherms were obtained at 77 K with a Micromeritics 2010. Before acquisition of the isotherm the sample was outgassed at 393 K under vacuum.

High-resolution synchrotron X-ray powder diffraction data of as-synthesized ECS-3 were collected at room temperature on the BM1B beamline at the synchrotron radiation source ESRF in Grenoble, during experiment CH-2699. The beamline was set to deliver a wavelength of 0.80175(2) Å. The borosilicate capillary (1.0 mm i.d.) containing the ECS-3 sample was spun during data collection to minimize preferred-orientation phenomena. Data were collected in continuous mode over the range $3 \le 2\theta \le 67°$ (accumulation times increased with increasing scattering angle) and were rebinned with a step size of 0.003° in 2θ.

ADT data were acquired with a Tecnai F30 S-TWIN transmission electron microscope equipped with a field-emission gun working at 300 kV. ADT data acquisition was performed with a FISCHIONE tomography holder by using the acquisition module described in reference [12a]. Crystal position was tracked by STEM images collected by a FISCHIONE high-angle annular dark-field detector (HAADF). Nano-electron diffraction was performed with a 10 μm C2 condenser aperture and a 70 nm beam. ADT data were collected in 1° steps. To improve reflection integration, the beam was precessed by a NanoMEGAS SpinningStar unit.[17] Electron-diffraction patterns were acquired with a CCD camera (14-bit GATAN 794MSC). The precession angle was kept at 1.2°. ADT-3D software was used for data processing, including geometrical parameter optimization, 3D diffraction-volume reconstruction, 3D visualization, automated cell-parameter determination, and intensity integration.[12b–c] E.s.d. for intensity was set to $\sqrt{\text{intensity}}$. Further details on the crystal structure investigations may be obtained from the Fachinformationszentrum Karlsruhe, 76344 Eggenstein-Leopoldshafen, Germany (fax: (+49) 7247-808-666; e-mail: crysdata@fiz-karlsruhe.de), on quoting the depository number CSD-423246.

Received: August 3, 2011
Published online: November 30, 2011

Keywords: electron diffraction · hydrothermal synthesis · organic–inorganic hybrid composites · structure elucidation · zeolite analogues

[1] *Introduction to Zeolite Science and Practice*, 3rd rev. ed. (Eds.: J. Čeika, H. van Bekkum, A. Corma, F. Schüth), Elsevier, Amsterdam, **2007**.
[2] G. Bellussi, A. Carati, E. Di Paola, R. Millini, W. O. Parker, Jr., C. Rizzo, S. Zanardi, *Microporous Mesoporous Mater.* **2008**, *113*, 252–260.
[3] F. Hoffmann, M. Cornelius, J. Morell, M. Fröba, *Angew. Chem.* **2006**, *118*, 3290–3328; *Angew. Chem. Int. Ed.* **2006**, *45*, 3216–3251.
[4] P. Wight, M. E. Davis, *Chem. Rev.* **2002**, *102*, 3589–3614.
[5] A. Corma, M. Iglesias, C. del Pino, F. Sanchez, *J. Chem. Soc. Chem. Commun.* **1991**, 1253–1254.
[6] Y. Yamamoto, Y. Nohara, Y. Domon, K. Takahashi, Y. Sakata, J. Plévert, T. Tatsumi, *Chem. Mater.* **2005**, *17*, 3913–3920.

[7] U. Díaz, J. A. Vidal-Moya, A. Corma, *Microporous Mesoporous Mater.* **2006**, *93*, 180 – 189.
[8] L. Su, M. Roussel, K. Vause, X. Y. Yang, F. Gilles, L. Shi, E. Leonova, M. Edén, X. Zou, *Microporous Mesoporous Mater.* **2007**, *105*, 49 – 57.
[9] F. Gramm, C. Baerlocher, L. B. McCusker, S. J. Warrender, P. A. Wright, B. Han, S. B. Hong, Z. Liu, T. Ohsuna, O. Terasaki, *Nature* **2006**, *444*, 79 – 81.
[10] C. Baerlocher, F. Gramm, L. Massüger, L. B. McCusker, Z. He, S. Hovmöller, X. Zou, *Science* **2007**, *315*, 1113 – 1116.
[11] C. Baerlocher, D. Xie, L. B. McCusker, S.-J. Hwang, I. Y. Chan, K. Ong, A. W. Burton, S. I. Zones, *Nat. Mater.* **2008**, *7*, 631 – 635.
[12] a) U. Kolb, T. Gorelik, C. Kübel, M. T. Otten, D. Hubert, *Ultramicroscopy* **2007**, *107*, 507 – 513; b) U. Kolb, T. Gorelik, M. T. Otten, *Ultramicroscopy* **2008**, *108*, 763 – 772; c) E. Mugnaioli, T. Gorelik, U. Kolb, *Ultramicroscopy* **2009**, *109*, 758 – 765.
[13] C. S. Birkel, E. Mugnaioli, T. Gorelik, U. Kolb, M. Panthöfer, W. Tremel, *J. Am. Chem. Soc.* **2010**, *132*, 9881 – 9889; I. Rozhdestvenskaya, E. Mugnaioli, M. Czank, W. Depmeier, U. Kolb, A. Reinholdt, T. Weirich, *Mineral. Mag.* **2010**, *74*, 159 – 177; I. Andrusenko, E. Mugnaioli, T. E. Gorelik, D. Koll, M. Panthöfer, W. Tremel, U. Kolb, *Acta Crystallogr. Sect. B* **2011**, *67*, 218 – 225; D. Denysenko, M. Grzywa, M. Tanigold, B. Streppel, I. Krkljus, M. Hirscher, E. Mugnaioli, U. Kolb, J. Hanss, D. Volkmer, *Chem. Eur. J.* **2011**, *17*, 1837 – 1848.
[14] M. C. Burla, R. Caliandro, M. Camalli, B. Carrozzini, G. L. Cascarano, L. De Caro, C. Giacovazzo, G. Polidori, R. Spagna, *J. Appl. Crystallogr.* **2005**, *38*, 381 – 388.
[15] C. Larson, R. B. Von Dreele, Los Alamos National Laboratory—Report LAUR-86-748, **2000**; B. H. Toby, *J. Appl. Crystallogr.* **2001**, *34*, 210 – 213.
[16] A. Corma, F. Rey, S. Valencia, J. L. Jorda, J. Rius, *Nat. Mater.* **2003**, *2*, 493 – 497.
[17] R. Vincent, P. A. Midgley, *Ultramicroscopy* **1994**, *53*, 271 – 282.

